electrode in the flowing bath solution, which were connected to a GeneClamp 500 amplifier (Axon Instruments, Foster City, CA) interfaced with a computer. A drop of water at 0°C, which was added to the recording chamber at the end of each experiment, produced the expected large depolarization mediated by Ca^{2+} and Cl^- channels [B. D. Lewis, C. Karlin-Neumann, R. W. Davis, E. P. Spalding, *Plant Physiol.* **114**, 1327 (1997)], a test of proper cell impalement.

15. D. J. Walker, R. A. Leigh, A. J. Miller, *Proc. Natl. Acad. Sci. U.S.A.* **93**, 10510 (1996).
16. The shunt resistance between an inserted electrode and the membrane permits a depolarizing current to flow [T. H. Goldsmith and M. H. M. Goldsmith, *Planta* **143**, 267 (1978)], the effect of which may be to underestimate V_m by 20 to 50 mV [W. Gassmann and J. I. Schroeder, *Plant Physiol.* **105**, 1399 (1994)]. Corrections of that magnitude would shift each of our V_m measurements, the most positive of which was −193 mV, to values more negative than −230 mV.
17. Plants were grown vertically on Petri plates containing 1.5% (w/v) agar, 1 mM KCl, and 1 mM $CaCl_2$ in continuous light for 4 to 5 days. Root protoplasts were prepared by cutting the root about 150 μm from the tip with a micromanipulator-mounted razor. The cut seedlings were infiltrated with an enzyme solution containing Cellulysin (12 mg/ml) (Calbiochem), Pectinase (2 mg/ml) (Sigma), and bovine serum albumin (5 mg/ml) (Sigma) dissolved in 10 mM KCl, 1 mM $CaCl_2$, 5 mM MES, and 300 mM sorbitol {pH 5.2 with 1,3-bis[tris(hydroxymethyl)methylamino]propane (BTP)} using a vacuum produced by a faucet aspirator. After 2 hours of incubation, the seedlings were rinsed in the solution without enzymes and stored at 4°C or placed in a 500- μl recording chamber containing 10 mM $CaCl_2$, 30 mM KCl, 5 mM Hepes, and 120 to180 mM sorbitol (pH 7.0 with BTP). Protoplasts of nonepidermal cells emerged from the cut end of the otherwise undigested root. Patch pipettes were filled with 130 mM K-glutamate, 2 mM EGTA, 5 mM Hepes, and 4 mM Mg–adenosine triphosphate (Mg-ATP) (pH 7.0 with BTP). Patch-clamp equipment and procedures were as described [M. H. Cho and E. P. Spalding *Proc. Natl. Acad. Sci. U.S.A.* **93**, 8134 (1996)]. Our procedures led to observations of inward currents in all patch-clamped wild-type cells. Lower percentages reported by others (*5*) may be explained by different growth conditions, different voltage protocols, or use of different tissue. We encountered more variability in the voltage dependence of the inward currents than has been reported for heterologously expressed inward rectifiers [F. Gaymard *et al.*, *J. Biol. Chem.* **271**, 22863 (1996)]. This variability is responsible for the appearance of weak rectification in the averaged whole-cell *I-V* curve in Fig. 3E. Channel gating may have been affected by cytoplasmic components that washed out in some patch-clamped protoplasts.
18. B. D. Lewis and E. P. Spalding, data not shown.
19. Patch pipettes were filled with 390 mM K-glutamate, 2 mM EGTA, 5 mM Hepes, and 4 mM Mg-ATP (pH 7.0 with BTP). The bath contained 130 mM KCl, 10 mM $CaCl_2$, and 5 mM Hepes (pH 7.0 with BTP). Tail currents were evoked by clamping V_m at −200 mV before stepping to a series of more positive potentials.
20. Plants were grown in continuous light on media containing KCl at the concentrations indicated plus 0.8% (w/v) agarose (Bio-Rad, Hercules, CA), 0.5% (w/v) sucrose, 2.5 mM $NaNO_3$, 2.5 mM $CaNO_3$, 2 mM $NH_4H_2PO_4$, 2 mM $MgSO_4$, 0.1 mM FeNaEDTA, 25 μM $CaCl_2$, 25 μM H_3BO_3, 2 μM $ZnSO_4$, 2 μM $MnSO_4$, 0.5 μM $CuSO_4$, 0.2 μM Na_2MoO_4, and 0.01 μM $CoCl_2$, adjusted to pH 5.7 with NaOH.
21. Of 104 seedlings tested, 23 were phenotypically scored as mutant and 88 were scored as wild type, giving $x^2 = 0.346$ (based on the expected ratio of three wild type to one mutant); $P > 0.05$.
22. Wild-type and *akt1-1* plants were grown on agar containing MS salts and 5% (w/v) sucrose in constant light for 14 days. Roots were excised, weighed, and washed for 16 to 17 hours in a K^+-free desorption solution (DS) containing 1.5 mM $CaCl_2$ adjusted to pH 5.7 with CaOH. Roots were incubated for 10 min in DS containing 4 mM NH_4Cl and 10 μM, 100 μM, or 1 mM Rb(^{86}Rb)Cl and then washed two times for 10 min each in ice-cold DS. Radioactivity was measured by detection of Cerenkov radiation.
23. J. I. Schroeder, J. M. Ward, W. Gassmann, *Annu. Rev. Biophys. Biomol. Struct.* **23**, 441 (1994); W. Gassmann, J. M. Ward, J. I. Schroeder, *Plant Cell* **5**, 1491 (1993).
24. Y. Cao, A. D. M. Glass, N. M. Crawford, *Plant Physiol.* **102**, 983 (1993); F. R. Vale, W. A. Jackson, R. J. Volk, *ibid.* **84**, 1416 (1987); F. R. Vale, R. J. Volk, W. A. Jackson, *Planta* **173**, 424 (1988).

25. Supported by the Department of Energy (DOE)/NSF/USDA Collaborative Research in Plant Biology Program (BIR-9220331), funds to R.E.H. from the NIH University of Wisconsin Cellular and Molecular Biology Training Grant (GM07215), to M.R.S. from DOE (DE-FG02-88ER13938) and NSF (DCB-90-04068), and to E.P.S. from the NASA/NSF Network for Research on Plant Sensory Systems (IBN-9416016). We thank T. Janczewski and R. Meister for technical assistance and P. Krysan, W. Robertson, J. Satterlee, and J. Young for helpful comments on the manuscript.

26 November 1997; accepted 27 March 1998

Knowing Where and Getting There: A Human Navigation Network

Eleanor A. Maguire,* Neil Burgess, James G. Donnett, Richard S. J. Frackowiak, Christopher D. Frith, John O'Keefe

The neural basis of navigation by humans was investigated with functional neuroimaging of brain activity during navigation in a familiar, yet complex virtual reality town. Activation of the right hippocampus was strongly associated with knowing accurately where places were located and navigating accurately between them. Getting to those places quickly was strongly associated with activation of the right caudate nucleus. These two right-side brain structures function in the context of associated activity in right inferior parietal and bilateral medial parietal regions that support egocentric movement through the virtual town, and activity in other left-side regions (hippocampus, frontal cortex) probably involved in nonspatial aspects of navigation. These findings outline a network of brain areas that support navigation in humans and link the functions of these regions to physiological observations in other mammals.

Where am I? Where are other places in the environment? How do I get there? Questions such as these reflect the essential functions of a navigation system. The neural basis of way-finding activity has been extensively studied. Spatially tuned neurons found in the hippocampal formation of freely moving rats [place cells coding for the rat's location (*1*) and head direction cells coding for its orientation (*2*)] support the idea that this part of the brain provides an allocentric (world-centered) representation of locations, or cognitive map (*3*). The posterior parietal lobe has been implicated in providing complementary egocentric representations of locations (centered on parts of the body) (*4*). Other brain regions, such as the dorsal striatum (*5*), have also been identified as possible elements of a navigation system. In humans, there has been much evidence for the involvement of the hippocampus in episodic memory, the memory for events set in their spatio-temporal context (*3*, *6*). By contrast, the role of the hippocampus in human navigation has remained controversial, and the wider neural network supporting human navigation is even less well understood. We attack this issue by combining functional neuroimaging with a quantitative characterization of human navigation within a complex virtual reality environment.

We used positron emission tomography (PET) (*7*) to scan subjects while they navigated to locations in a familiar virtual reality town using their internal representation of the town built up during a continuous period of exploration immediately before scanning (Fig. 1A). In one navigation condition, the subjects could head directly toward the goal (nav1), while in the other (nav2), direct routes were precluded by closing some of the doors and placing a barrier to block one of the roads, forcing the subjects to take detours. Navigation was compared to a task in which subjects moved through the town following a trail of arrows, thus not needing to refer to an internal representation of the town. An additional task requiring the identification of features in static scenes from the town was included for contrast with the three dynamic tasks (*8*).

We first investigated which brain regions were involved in successful naviga-

E. A. Maguire, R. S. J. Frackowiak, C. D. Frith, Wellcome Department of Cognitive Neurology, Institute of Neurology, University College London, 12 Queen Square, London WC1N 3BG, UK.
N. Burgess, J. G. Donnett, J. O'Keefe, Department of Anatomy and Developmental Biology and Institute of Cognitive Neuroscience, University College London, Gower Street, London WC1E 6BT, UK.

*To whom correspondence should be addressed. E-mail: e.maguire@fil.ion.ucl.ac.uk

tion in both direct and detour way-finding. The trials in these conditions were divided into successful ones in which the correct destination was reached (22/30 trials in nav1 and 21/30 in nav2 across the 10 subjects) and those in which it was not. The successful trials compared to the arrows task showed significant activation of the right hippocampus (Fig. 1B), as did the comparison of the successful trials with the unsuccessful trials. This latter comparison also revealed activation in the left hippocampus, left lateral temporal cortex, left frontal cortex, and in the thalamus (Fig. 1B).

In order to explore in greater depth the relationship between regional cerebral blood flow (rCBF) and behavior during direct way-finding (nav1), we derived a quantitative measure of the accuracy of heading toward the goal (9). The accuracy of heading measured across all trials in nav1 covaried significantly with rCBF in the right hippocampus and the right inferior parietal cortex (Fig. 2). Not only is the right hippocampus more active during navigation than trail-following, but the more accurate the navigation, the more active it is.

These results are consistent with our interpretation that the right hippocampus and inferior parietal cortex cooperate to enable navigation to an unseen goal: The hippocampus provides an allocentric (environment-based) representation of space that allows the computation of the direction from any start location to any goal location, and the right inferior parietal cortex uses this information to compute the correct body turns to enable movement toward the goal given the relative (egocentric, body-centered) location of obstacles in the way (doorways to go through, barriers across roads, and so forth) and the current heading direction. Because the parietal cortex takes account of information in addition to the allocentric direction to the goal, it would not have as high a correlation with the accuracy of heading toward the goal as the hippocampal formation (consistent with our findings; Fig. 2). Similarly, rCBF in the right inferior parietal cortex would not be significantly different in the trail-following and way-finding conditions, because both tasks have similar egocentric requirements, and no such difference was found (Fig. 1B). However, differences in right inferior parietal activity would be expected when subtracting the static condition from either trail-following or way-finding. This comparison did indeed show right inferior parietal activation, along with bilateral activation of medial parietal areas, which we assume are also involved in egocentric aspects of movement, for example, processing the optic flow generated by the movement (Fig. 3B) (*10*).

Activity in the left hippocampus, although associated with successful navigation, does not covary significantly with our measure of the accuracy of navigation. We interpret this as a role in actively maintaining the memory trace of the appropriate destination during navigation or recollecting specific paths taken during learning that lead to the goal but are not necessarily direct. Either role would be consistent with the known involvement of the left hippocampus in "episodic" memory for personally experienced events (*6*).

These results are consistent with previous reports of the involvement of the hippocampal or parietal areas in topographical memory (*11*) and provide a more precise interpretation of their roles in the actual performance of navigation.

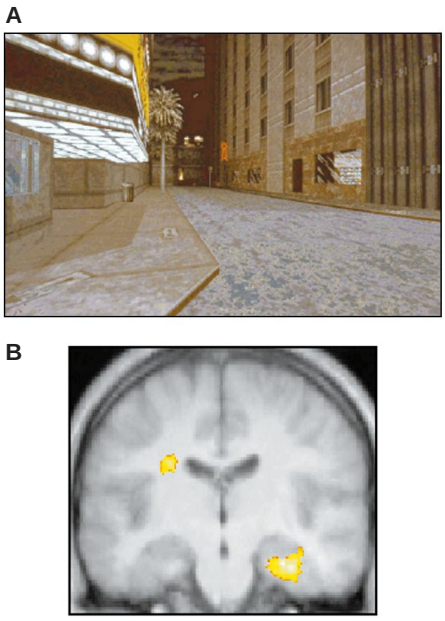

Fig. 1. (**A**) Example of view from inside the virtual town. (**B**) The comparison between successful navigation (nav1 and nav2) compared to following a trail of arrows. PET data are superimposed onto the averaged MRI of the 10 subjects at the voxel of peak activation in the right hippocampus displayed in the coronal plane. The color scale of the activation pertains to the significance level of the *z* scores with the peak of the activation in white. Coordinates in stereotactic space (*x,y,z*, respectively) and *z* scores of the activations are: right hippocampus (30, −16, −22; $z = 3.74$) and left tail of caudate (−28, −16, 28; $z = 3.05$). Other areas activated in this comparison but not displayed on this plane were: left occipital area 18 (−24, −102, −2; $z = 3.50$) and left superior frontal gyrus (−22, 52, 22; $z = 3.65$). The comparison between successful versus lost trials showed the following activations: right hippocampus (30, −20, −16; $z = 3.61$); left hippocampus (−16, −26, −6; $z = 4.10$); left superior temporal gyrus (−54, −30, 14; $z = 3.86$); left inferior temporal gyrus (–52, −50, −12; $z = 5.23$); left inferior frontal gyrus (–46, 22, 6; $z = 4.59$); and right thalamus (6, −6, 12; $z = 4.25$).

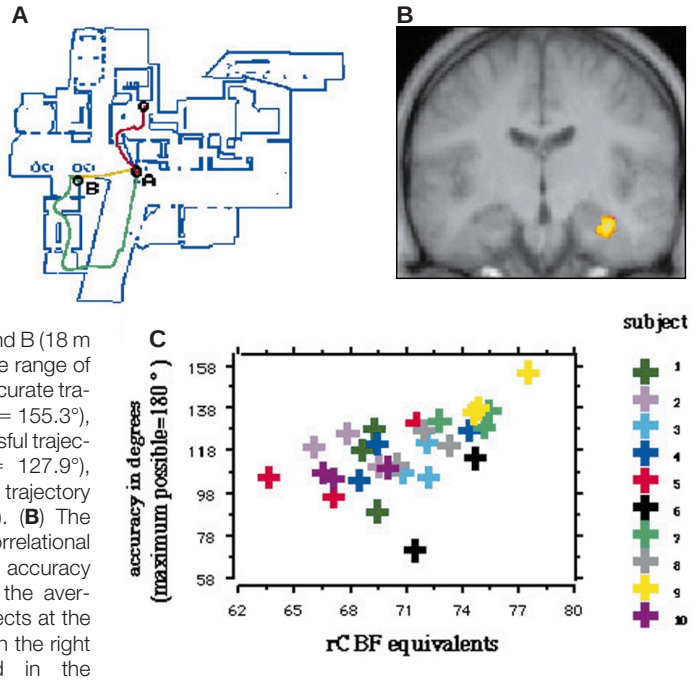

Fig. 2. (**A**) The virtual environment is shown from an aerial perspective, demonstrating the complexity of the town and the many possible paths between the various places. Subjects' navigation during scanning on the navigation task was analyzed in terms of accuracy in degrees (*9*). Three trajectories between the screens at A and B (18 m apart) are shown from the range of subjects' behavior: an accurate trajectory (yellow, accuracy = 155.3°), an inaccurate but successful trajectory (green, accuracy = 127.9°), and an inaccurate "lost" trajectory (red, accuracy = 70.6°). (**B**) The PET data from the correlational analysis of rCBF (*22*) and accuracy are superimposed onto the averaged MRI of the 10 subjects at the voxel of peak activation in the right hippocampus displayed in the coronal plane. Areas activated in this comparison were right hippocampus (36, –12, –20; $z = 3.66$; displayed in figure) and right inferior parietal cortex (60, –30, 50; $z = 3.36$). (**C**) Scatter plot of the correlation of rCBF values at the voxel of peak activation in the right hippocampus plotted against the accuracy of navigation ($r = 0.56$, $P < 0.002$). The behavioral data for one trial of one subject (subject 6) was not available. The data points for each subject are plotted in different colors. The correlation of accuracy of navigation and perfusion in the right inferior parietal cortex was $r = 0.43$, $P < 0.02$.

Next, we looked at successful navigation requiring detours (nav2) compared to successful navigation in the nav1 condition. This comparison revealed left frontal activation (Fig. 3A). The increased requirement for strategy switching in the presence of obstacles (nav2) compared to direct way-finding (nav1) is consistent with findings of frontal involvement in other studies with tasks making similar demands (*12*). Left frontal activation was also apparent when successful navigation was compared to following arrows or compared to unsuccessful navigation. These frontal activations are consistent with a role for this region in planning and decision making (*13*). It is likely that following the trail of arrows demands less planning than way-finding.

As well as comparing the dynamic and static tasks detailed above, we further characterized movement in the town in terms of the speed of motion, that is, the ratio between distance traveled and time taken, producing an average speed measure in virtual meters per second. In contrast to the areas whose activity correlated with navigational accuracy, the only area of regional activation that covaried significantly with speed of navigation in the nav1 condition was in the right caudate nucleus; rCBF in this region increased as speed increased (Fig 3, C and D). This correlation with speed of virtual navigation was much more significant than that with simple motor response variables such as the rate or average duration of keypad presses (Fig. 3D). It suggests a higher function than the simple control of the physical movement of parts of the body, although its precise interpretation remains open. The dorsomedial caudate region receives projections from the cortices adjacent to the hippocampus in rats (*14*). We suggest that location within the environment or spatial context might provide an important source of information for the striatal control of higher-level aspects of current or planned movements and that this control is reflected in the amplitude or speed of movement, rather than the direction of movement.

In conclusion, our results outline the network of brain regions supporting human navigation and suggest specific roles for each of these regions. They agree with, and further illuminate, previous findings showing that lesions of the right human hippocampus result in deficits of spatial memory (*15*) while those of the right inferior parietal cortex result in deficits of the ability to represent or act on objects located with respect to the egocentric left-right body axis (*16*). Our interpretation of the parietal role in navigation agrees with neuronal responses from inferior parietal cortex in monkeys (in particular, area 7a and the lateral intraparietal area) implicating it in the translation of the location of stimuli from retinal to head- or body-centered coordinates (*4*), and with the connections of area 7a to the hippocampal formation [including the presubiculum which, at least in rats, codes for the current head direction (*2*)]. Our interpretation of the hippocampal role in navigation is concordant with neuronal responses in rats (*3*) and with models of how the hippocampus guides rats' navigation (*17*), from which our measure of navigational accuracy was explicitly derived. Our finding that rCBF in the right caudate nucleus correlates with the speed of navigation is compatible with its proposed role in motor learning (*18*) and the process by which movements are reinforced [and hence, the occurrence of abulia after lesions of this region (*19*)], and also with the more general hypothesis of a role in context recognition (*20*). It also has relevance to the suggestions that rats may use signals derived from cells that encode their speed of movement to determine distances and that such speed cells might be located in one of the sub-cortical nuclei (*21*), perhaps in the basal ganglia as we identified here. Although many details of the inputs and outputs of a human navigation network remain to be specified, we have demonstrated the closest link yet between humans and other mammals in the neural implementation of navigation.

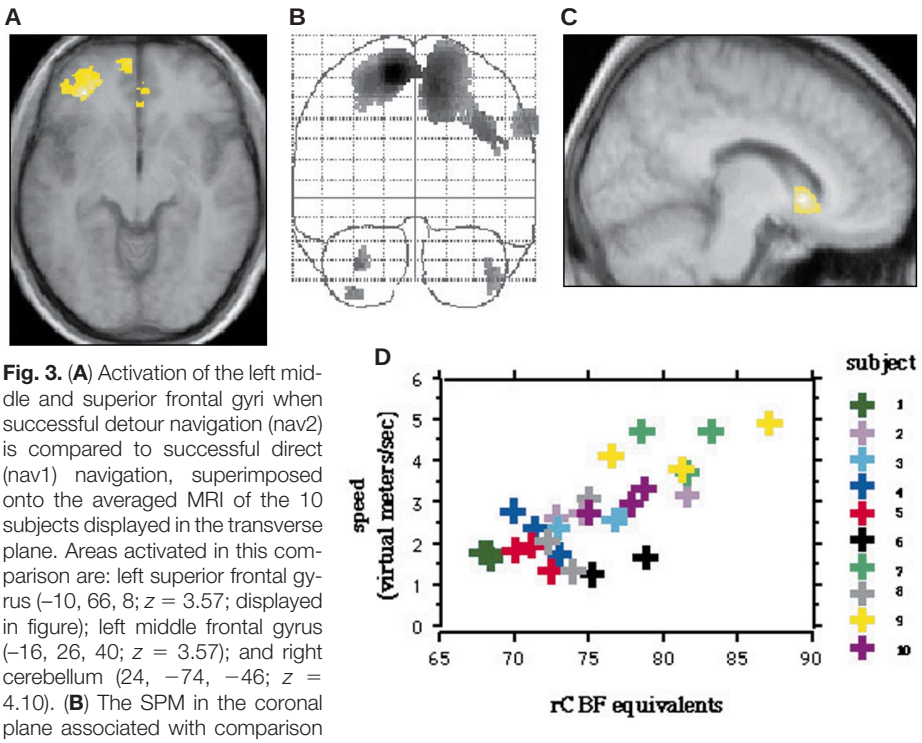

Fig. 3. (**A**) Activation of the left middle and superior frontal gyri when successful detour navigation (nav2) is compared to successful direct (nav1) navigation, superimposed onto the averaged MRI of the 10 subjects displayed in the transverse plane. Areas activated in this comparison are: left superior frontal gyrus (–10, 66, 8; $z = 3.57$; displayed in figure); left middle frontal gyrus (–16, 26, 40; $z = 3.57$); and right cerebellum (24, −74, −46; $z = 4.10$). (**B**) The SPM in the coronal plane associated with comparison of movement tasks (nav1, nav2, arrows) with the static scenes task. Displayed on a transparent brain to facilitate viewing of all significant activations that are on different planes. Areas activated: left medial parietal cortex (−16, −52, 54; $z = 4.48$); right medial parietal cortex (12, −68, 48; $z = 4.02$); right inferior parietal lobe (56, −38, 32; $z = 6.30$); left cerebellum (−34, −40, −40; $z = 3.89$); and right cerebellum (49, −36, −38; $z = 4.22$). (**C**) Activity in the right caudate covaried significantly with speed of virtual movement, displayed here in sagittal section on the averaged MRI of the 10 subjects at the voxel of peak activation in the right caudate (10, 14, −4; $z = 3.97$). (**D**) Scatter plot of the correlation of rCBF (*22*) values at the voxel of peak activation in the right caudate plotted against the speed of navigation ($r = 0.75$, $P < 0.0001$). The behavioral data for one trial of one subject (subject 6) was not available. The data points for each subject are plotted in different colors. The correlations between right caudate rCBF and peripheral motor behaviors were much less significant (average duration of button press $r = 0.08$, $P < 0.67$; rate of button pressing $r = 0.51$, $P < 0.004$).

REFERENCES AND NOTES

1. J. O'Keefe and J. Dostrovsky, *Brain Res.* **34**, 171 (1971).
2. J. S. Taube, R. U. Muller, J. B. Ranck, *J. Neurosci.* **10**, 420 (1990).
3. J. O'Keefe and L. Nadel, *The Hippocampus as a Cognitive Map* (Clarendon, Oxford, 1978).
4. R. A. Anderson, *Philos. Trans. R. Soc. London Ser. B* **352**, 1421 (1997); H. O. Karnath, *ibid.*, p. 1411; G. Vallar, *ibid.*, p. 1401.
5. S. I. Wiener, *J. Neurosci.* **13**, 3802 (1993); B. D. Devan, E. H. Goad, H. L. Petri, *Neurobiol. Learn. Mem.* **66**, 305 (1996); M. Potegal, *Spatial Abilities: Development and Physiological Foundations* (Academic Press, New York, 1982).
6. M. Kinsbourne and F. Wood, in *Short-Term Memory*, D. Deutsch and J. A. Deutsch, Eds. (Academic Press, New York, 1975), pp. 257–291; E. Tulving, *Elements of Episodic Memory* (Clarendon, Oxford, 1983); F. Vargha-Khadem *et al.*, *Science* **277**, 376 (1997); B. Milner, *Clin. Neurosurg.* **19**, 421 (1972).
7. Ten healthy right-handed male subjects (mean age,

36.5 years) participated in the study, approved by the local hospital ethics committee and the UK Administration of Radioactive Substances Advisory Committee. Each subject had 12 PET scans. There were four tasks each performed three times in a counterbalanced order. PET scans were obtained using a Siemens/CPS ECAT EXACT HR+ (model 962) PET scanner. Scanning was performed with septa retracted, in three-dimensional (3D) mode. The field of view of 15.5 cm in the axial extent allowed the whole brain to be studied. Volunteers received an $H_2{}^{15}O$ intravenous bolus (330 MBq) infused over 20 s followed by a 20-s saline flush through a forearm cannula. Data were acquired in a 90-s scan frame. There were 12 successive administrations of $H_2{}^{15}O$, each 8 min apart. The integrated radioactivity counts that accumulated over the 90-s acquisition period, corrected for background, were used as an index of regional cerebral blood flow. Attenuation correction was computed with a transmission scan before emission scan acquisition. Images were reconstructed into 128 pixels by 128 pixels in 63 planes with an in-plane resolution of 6.5 mm. In addition, high-resolution magnetic resonance imaging (MRI) scans were obtained with a 2.0-T Vision system (Siemens GmbH, Erlangen, Germany) using a T1-weighted 3D gradient echo sequence. The image dimensions were 256 voxels by 256 voxels by 256 voxels. The voxel size was 1 mm by 1 mm by 2 mm. Images were analyzed with Statistical Parametric Mapping (SPM'96, Wellcome Department of Cognitive Neurology, London, UK; www.fil.ion.ucl.ac.uk) executed in MATLAB (Mathworks, Sherborn, MA). All scans were automatically realigned to the first scan and then normalized using a nonlinear deformation [K. J. Friston *et al.*, *Hum. Brain Mapp.* **2**, 189 (1995)] into standard stereotactic space [J. Talairach and P. Tournoux, *Co-Planar Stereotactic Atlas of the Human Brain* (Thieme, Stuttgart, Germany, 1988)] using a template from the Montreal Neurological Institute [A. C. Evans *et al.*, in *Proceedings of the IEEE-Nuclear Science Symposium and Medical Imaging Conference*, San Francisco, CA, 31 October to 6 November 1993, L. A. Klaisner, Ed. (IEEE Service Center, Piscataway, NJ, 1993), pp. 1813–1817]. The structural MRI scans were normalized into the same space to allow for the superimposition of PET activations onto an averaged structural image. Images were smoothed using an isotropic Gaussian kernel of 16 mm (full width at half maximum) to optimize the signal-to-noise ratio and to adjust for intersubject differences in gyral anatomy. Global variance between conditions was removed, using analysis of covariance (ANCOVA). For each pixel in stereotactic space, condition-specific adjusted rCBF values with an associated adjusted error variance were generated. Areas of significant change in brain activity were then determined, using appropriately weighted contrasts between the task-specific scans and the *t* statistic. The resulting sets of *t* values constituted the statistical parametric map (SPM). Significance levels were set at $P < 0.001$ (uncorrected).

8. A commercially available computer game (Duke Nukem 3D, 3D Realms Entertainment, Apogee Software Ltd., Garland, TX) was used to present the virtual reality town on a 120-MHz Pentium-based personal computer, showing a color, 3D, fully textured first-person view. The town was created using the editor provided (BUILD, Ken Silverman, 3D Realms Entertainment). The game's record and playback functions were used to store subjects' actions and replay them for subsequent analysis. The town had four streets and contained shops, bars, a cinema, church, bank, train station, and video games arcade (Fig. 1A). Subjects could enter into and navigate through the buildings, as each room had at least two entrances. The town contained small screens on the walls at various locations. Approaching a screen and switching it on caused it to display a view of another part of the town. Subjects controlled their movement within the environment by using a keypad with backward, forward, left turn, and right turn buttons. A fifth button served to activate screens. Before scanning acquisition, subjects spent up to 60 min exploring the environment until they felt that they had learned the spatial layout of streets and building interiors. A trail of arrows on the floor was present during exploration and in all conditions, but was only relevant in the arrows condition. Subjects were scanned under four conditions. (i) nav1: subjects switch on a screen and navigate through the town to the destination displayed. When the destination is reached, the subject activates the screen found there, which displays the next destination, and so on; (ii) nav2: identical to nav1, except that some doors have been closed, and a barrier has been moved to block a different street; (iii) arrows: subjects move through the town following a trail of arrows on the floor. Subjects activated the screens encountered during the task, but the views of the town displayed had no relevance to their task; (iv) scenes: static scenes from the town are presented every 2 s, subjects respond according to whether there is a screen in the scene or not.
9. For the nav1 condition, the subject's heading direction θ_h (in degrees) and the direction of the current destination θ_d were calculated at each meter along the subject's trajectory. The absolute difference $|\theta_h - \theta_d|$ was found at each meter and was averaged over a trial to give $A = 180 - \langle|\theta_h - \theta_d|\rangle$ as a measure of accuracy of heading. Similar analysis was not applied to the nav2 detour condition, because subjects did not know beforehand which doors would be closed or where the barriers would be, and so could not be expected to plan an optimal route. Theoretically, accuracy scores may vary from 0 (always moving directly away from the current destination), through 90° (moving randomly) to 180° (always moving directly toward the current destination). In practice, an accuracy of 160° is hard to exceed because of the cluttered nature of the environment (the accuracy of one very well-practiced author, N.B., in the three trials varied between 144.3° and 157.4°). This measure agrees with our subjective assessment of trials, was independent of the speed of navigation, and is consistent with models of how the hippocampus directs navigation in rodents (*17*).

10. B. M. DeJong, S. Shipp, B. Skidmore, R. S. J. Frackowiak, S. Zeki, *Brain* **117**, 1039 (1994).
11. G. K. Aguirre, J. A. Detre, D. C. Alsop, M. D'Esposito, *Cereb. Cortex* **6**, 823 (1996); E. A. Maguire, R. S. J. Frackowiak, C. D. Frith, *Proc. R. Soc. London Ser. B* **263**, 1745 (1996); O. Ghaem *et al.*, *Neuroreport* **8**, 739 (1997); E. A. Maguire, R. S. J. Frackowiak, C. D. Frith. *J. Neurosci*. **17**, 7103 (1997); G. K. Aguirre and M. D'Esposito, *ibid.*, p. 2512; E. A. Maguire, C. D. Frith, N. Burgess, J. G. Donnett, J. O'Keefe, *J. Cogn. Neurosci*. **10**, 61 (1998).
12. A. Bechara, D. Tranel, H. Damasio, A. R. Damasio, *Cereb. Cortex* **6**, 215 (1996); R. Elliott, C. D. Frith, R. J. Dolan, *Neuropsychologia* **35**, 1395 (1997).
13. A. R. Luria, *Higher Cortical Functions in Man* (Tavistock, London, 1966); B. Milner, *Arch. Neurol.* **9**, 90 (1963); T. Shallice, *Philos. Trans. R. Soc. London Ser. B* **298**, 199 (1982).
14. A. E. Kelly and V. B. Domesick, *Neuroscience* **7**, 615 (1982); L. W. Swanson and C. Kohler, *J. Neurosci.* **6**, 3010 (1986); A. J. McGeorge and R. L. M. Faull, *Neuroscience* **29**, 503 (1989).
15. E. A. Maguire, T. Burke, J. Phillips, H. Staunton, *Neuropsychologia* **34**, 993 (1996); M. L. Smith and B. Milner, *ibid.* **19**, 781 (1981).
16. N. Burgess, J. G. Donnett, K. J. Jeffery, J. O'Keefe, *Philos. Trans. R. Soc. London Ser. B* **352**, 1397 (1997).
17. J. O'Keefe, *Brain and Space*, J. Paillard, Ed. (Oxford Univ. Press, Oxford, 1991), pp. 273–295; N. Burgess and J. O'Keefe, *Hippocampus* **6**, 749 (1996).
18. R. E. Passingham, in *Neural and Behavioral Approaches to Higher Brain Functions*, S. Wise, Ed. (Wiley, New York, 1987); R. E. Passingham, *The Frontal Lobes and Voluntary Action* (Oxford Univ. Press, Oxford, 1995).
19. K. P. Bhatia and C. D. Marsden, *Brain* **117**, 859 (1994).
20. J. C. Houk and S. P. Wise, *Cereb. Cortex* **5**, 95 (1995).
21. J. O'Keefe, N. Burgess, J. Donnett, E. A. Maguire, *Philos. Trans. R. Soc. London Ser. B*, in press.
22. C. Buchel, R. S. J. Wise, C. J. Mummery, J. B. Poline, K. J. Friston, *Neuroimage* **4**, 60 (1996).

23. E.A.M., R.S.J.F., and C.D.F. are supported by the Wellcome Trust, J.O'K. and J.G.D. by the Medical Research Council, and N.B. by the Royal Society. We thank K. Friston, C. Price, and C. Buchel for helpful comments.

11 December 1997; accepted 20 March 1998